Geophys. J. Int. (1996) **127**, 515–528

Determination of the isotropic component of deep focus earthquakes by inversion of normal-mode data

Tatsuhiko Hara,[1] Keiko Kuge[2] and Hitoshi Kawakatsu[1]

[1] *Earthquake Research Institute, Tokyo University, Tokyo* 113, *Japan*

[2] *Department of Geophysics, Faculty of Science, Kyoto University, Kyoto* 606-01, *Japan*

Accepted 1996 July 1. Received 1996 June 28; in original form 1996 January 2

SUMMARY

We determine the isotropic component of large deep earthquakes by inversion for their full six-component moment tensors using the normal-mode data. We show that it is possible to reduce the correlation between the isotropic component and other components and to determine the isotropic component independently by analyses of normal-mode data at periods longer than 500 s. We find no significant isotropic component for the earthquakes we studied; the magnitudes of the estimated isotropic components are comparable to the uncertainty due to the mislocation of the centroid. The magnitude of the isotropic component is at most 5 per cent of the deviatoric seismic moment if it exists. This suggests that, if a rapid phase change of mantle minerals occurs during the rupture of deep earthquakes, the mantle material that transformed would be confined within an extremely thin layer.

We also conduct moment tensor inversion using body waves and surface waves in the period band between 20 and 500 s. We find that there is a relatively consistent non-double-couple component of the deviatoric moment tensor for the Japan Sea earthquake (1994 July 21). This is likely to be caused by source complexity

Key words: deep focus earthquakes, earthquake-source mechanism, global seismology, inversion, long period, normal modes.

1 INTRODUCTION

Precise estimation of the moment tensors of deep focus earthquakes is important for understanding their physical mechanisms. Since an isotropic component could be due to a volumetric change associated with a rapid phase transformation, whether or not deep earthquakes have significant isotropic components has important geophysical implications. Although many studies have tried to identify non-zero isotropic components (e.g. Dziewonski & Gilbert 1974; Gilbert & Dziewonski 1975), no significant isotropic component of deep earthquakes has ever been observed (e.g. Okal & Geller 1979; Vasco & Johnson 1989; Kawakatsu 1991, 1996).

As has been suggested by previous studies (Mendiguren & Aki 1978; Kawakatsu 1991, 1996), the difficulty in identifying the isotropic component primarily comes from the fact that the radiation of seismic waves due to the isotropic component is very similar to that due to the vertical CLVD component (Randall & Knopoff 1970). There are two data sets that make it possible to resolve these components. One is long-period body-wave data, containing *P*, *PP*, *SP*, *SS* and other phases (Kawakatsu 1991, 1996). This data set has good coverage of the focal sphere, and is suitable for determining the isotropic component independently from the other components. Kawakatsu (1991, 1996) conducted CMT inversion of long-period body-wave data in the period band between 50 and 100 s, and showed that there was no significant isotropic component for the deep earthquakes he studied.

The second data set, which was suggested by Kawakatsu (1996), is normal-mode data at periods longer than 500 s. The variation of the relative excitation of normal modes due to the isotropic component and the vertical CLVD component makes it possible to resolve these components independently. In our previous study (Hara, Kuge & Kawakatsu 1995; hereafter referred to as Paper I), we investigated whether the 1994 Bolivia earthquake had a significant isotropic component using normal-mode data. We showed, by checking the correlation matrix (Fig. 3d in Paper I), that it was possible to determine the isotropic component independently from the other components using normal-mode data in the period band between 550 and 1000 s. We examined the effect of the error of the centroid location and 3-D earth structure, and found no significant isotropic component for the Bolivia earthquake.

One of the merits of the normal-mode analysis is that we can obtain the moment tensor solution at long periods, which may reveal possible slow source processes that cannot be

detected using shorter-period body-wave data. Another advantage is the large variance reduction. For example, in Paper I, 94.4 per cent of the total variance of the normal-mode data is accounted for by the synthetic seismograms computed for the moment tensor solution. This suggests that the bias due to unmodelled earth structure is small. In addition, we can include the effect of 3-D earth structure exactly by computing synthetics using the direct solution method (DSM, Geller *et al.* 1990; Hara, Tsuboi & Geller 1991, 1993), so we can investigate the effect of 3-D earth structure on the estimation of the isotropic component.

The main purpose of the present paper is to investigate whether other deep earthquakes have significant isotropic components by analysis of their normal-mode data. We first explain how we estimate the isotropic component and its uncertainty using the analyses for the Bolivia earthquake as an example, since the most detailed investigation can be made for this earthquake. As we show below, the correlation between the isotropic component and the other components has a large impact on estimates of the isotropic component; special attention should be paid to this point. This effect has not been carefully considered by previous studies of the isotropic component of deep earthquakes using normal-mode data, except for our study of the 1994 Bolivia earthquake.

We then perform inversion for the full six components of the moment tensors of large deep earthquakes using normal-mode data, and investigate whether significant isotropic components are observed.

In addition to our analyses of normal-mode data, we perform moment tensor inversion using body waves and surface waves in the period band between 20 and 500 s, and investigate whether significant non-double-couple components of the deviatoric moment tensor are observed.

2 RE-DEFINITION OF THE MOMENT TENSOR

In order to show clearly the correlation between the isotropic component and other components, following Kawakatsu (1991), we redefine the diagonal components of the moment tensors as follows:

$$I=(M_{rr}+M_{\theta\theta}+M_{\phi\phi})/3,$$

$$C=(-2M_{rr}+M_{\theta\theta}+M_{\phi\phi})/3,$$

$$D=(M_{\theta\theta}-M_{\phi\phi})/2,$$

where I is the isotropic component and C is a vertical compensated linear vector dipole (CLVD) (Randall & Knopoff 1970).

The 'non-double-couple component' of the moment tensor, ε, is defined as follows:

$$\varepsilon=-\frac{(e_2-I)}{\max(|e_1-I|, |e_3-I|)}, \quad (1)$$

where e_i represents an eigenvalue of the moment tensor ($e_1 \geq e_2 \geq e_3$). When the isotropic component is zero, this is the same as the quantity defined by Giardini (1983, 1984).

3 DATA AND ANALYSES

3.1 Normal-mode analyses

We choose the large deep earthquakes shown in Table 1 for the normal-mode analyses. We employ IDA seismograms for the 1982 Banda Sea (June 22) and the 1984 South of Honshu (March 6) earthquakes, and IRIS broad-band seismograms for the 1994 Fiji (March 9), Bolivia (June 9), and Japan Sea (July 21) earthquakes. The duration of the seismograms is 10 hours for the 1982 Banda Sea, 1984 South of Honshu and 1994 Bolivia earthquakes, and 5 hours for the 1994 Fiji and Japan Sea earthquakes. We employ relatively short time-series compared to the usual normal-mode analyses to reduce the effect of 3-D earth structure on observed waveform data. We do not use the first portions of the IDA seismograms to avoid using seismograms contaminated by non-linearity of the instrument response.

For the moment, we fix the centroid location using the Harvard CMT solutions. We investigate the effect of varying the centroid location below. We use Model 1066A (Gilbert & Dziewonski 1975) as the earth model, and compute Green's function using the DSM. In the DSM, the wavefield is expressed as a linear combination of trial functions. We choose the eigenfunctions of all of the degenerate singlets of the multiplets of 1066A whose eigenperiods are larger than 350 s as trial functions. We fully consider coupling between trial functions due to the earth's rotation and its elliptical figure in calculating the potential and kinetic energy matrix. We assume that the source time function is a step function.

Kawakatsu (1996) showed that the sign of the correlation between the isotropic component and the vertical CLVD component varies significantly at periods longer than 500 s, and suggested that it is possible to determine the isotropic and vertical CLVD components independently using normal-mode data in this period range. We explain the reasons in terms of the excitation of normal modes in the Appendix.

3.2 Broad-band analyses

We perform broad-band analyses for the 1994 Fiji, Bolivia, and Japan Sea earthquakes using IRIS broad-band seismograms. We conduct three analyses for each earthquake. In the first analysis, we use the first portions of the observed seismograms, which contain the *P* wavetrain (*P*, *pP*, *sP*, *PP*) and *SH* waves in the period band between 20 and 250 s. The duration of the time-series employed for each earthquake is listed in Table 2. We perform inversion for the moment tensors and

Table 1. The event list (after Harvard).

Event	Date	Latitude	Longitude	Depth (km)	Seismic moment (N·m)
Banda Sea	82/06/22	7.28S	125.99E	473	1.8×10^{20}
South of Honshu	84/03/06	29.60N	139.11E	446	1.4×10^{20}
Fiji	94/03/09	17.71S	178.11W	573	2.8×10^{20}
Bolivia	94/06/09	13.81S	67.20W	657	3.0×10^{21}
Japan Sea	94/07/21	42.30N	132.83E	478	9.7×10^{19}

Table 2. The duration of the time-series employed in analyses of *P* wavetrains and *SH* waves.

Event	Data	
	P wavetrains	SH waves
Bolivia	300 s	60 s
Fiji	280 s	60 s
Japan Sea	200 s	40 s

source time functions using this data set. The inversion scheme follows that of Kuge & Kawakatsu (1993).

In the second analysis, using the portions of seismograms from the first *P*-wave arrivals to just before the Love-wave arrivals, we conduct CMT inversion of long-period body-wave data in the period band between 50 and 100 s. The third analysis is CMT inversion of long-period surface-wave data. We use the period band between 250 and 500 s for the Bolivia earthquake, and 140 and 290 s for the Fiji and Japan Sea earthquakes, respectively. The duration is about 3000 s; the waveforms include G1 and R1. In the second and third analyses, we use 1066A as an earth model, and assume that the source time function is a step function. While the location of the earthquake is fixed in the first analysis, it is treated as an unknown in the second and third analyses.

It is possible to form an estimate of the reliability of the non-double-couple component (ε) based on the consistency between solutions determined for the different data sets (e.g. Kuge & Kawakatsu 1990). Since each data set is sensitive to a different portion of the earth structure, and since the correlation between the components of the moment tensor is different in each analysis, the consistent and large value of the (deviatoric) non-double-couple component (ε) suggests that this is not an artefact due to large-scale 3-D structure or the instability of the inversion procedure.

4 1994 BOLIVIA DEEP EARTHQUAKE

We first present the results of the analyses for the 1994 Bolivia earthquake. Table 3 shows the moment tensor solutions obtained by each analysis. We show the solution obtained by

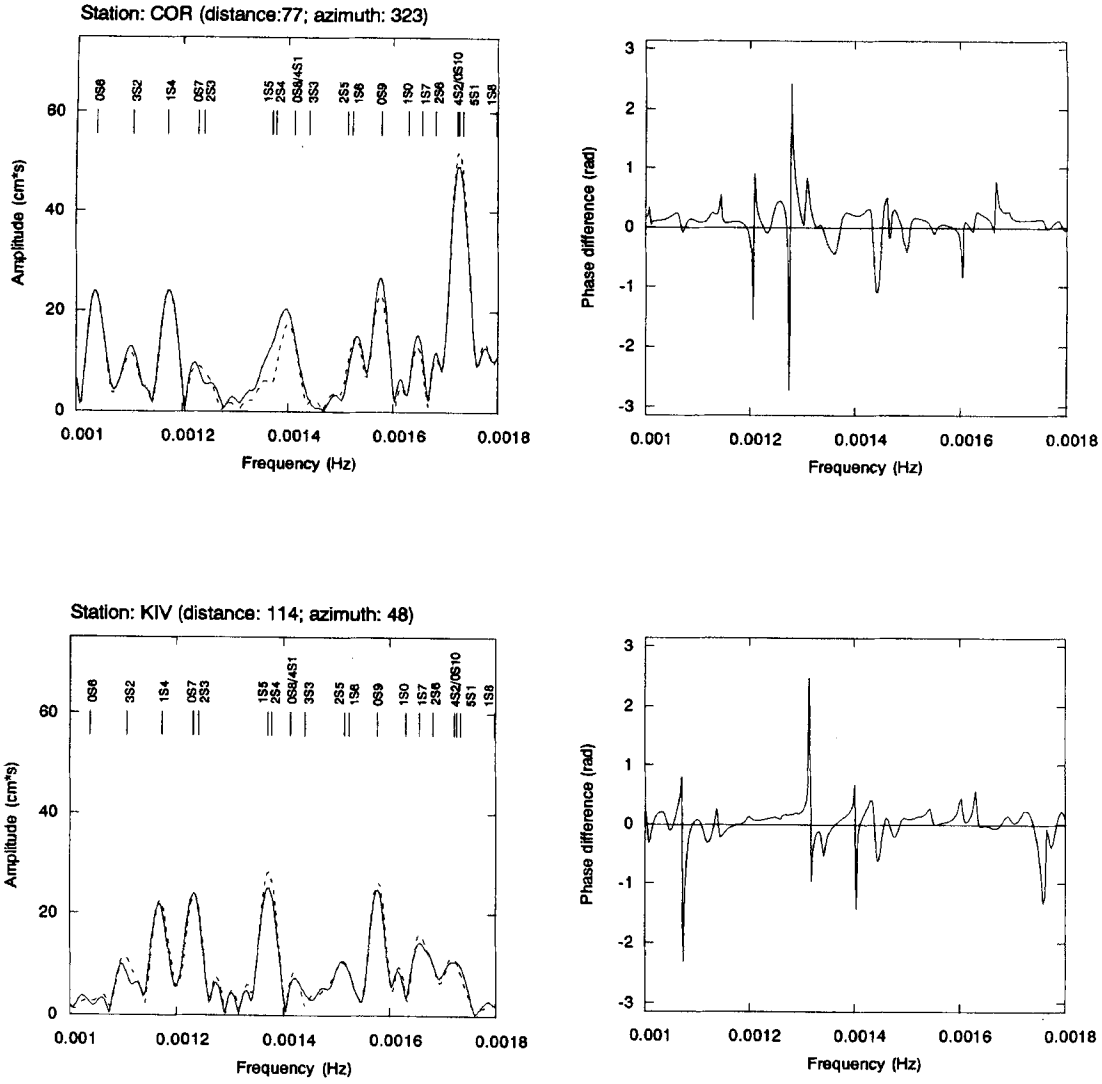

Figure 1. Comparison between observation and synthetics. The left panels show the amplitude spectra (solid curves: observed; dashed curves: synthetic). The vertical bars in the left panels indicate the eigenfrequencies of the normal modes computed for 1066A. The right panels show the phase differences between the observed and synthetic spectra.

the analysis of the normal-mode data in the period band between 550 and 1000 s in Table 3. We explain later the reason why we chose this period band and solution. The moment tensor of the Bolivia earthquake is primarily a double couple; the isotropic component, which is specified as a percentage of the deviatoric seismic moment, and the non-double-couple component (ε) are small for each of the analyses.

Although its magnitude is larger than two standard deviations, the isotropic component estimated by the normal-mode analyses is not significant because, as we show below, the actual uncertainty is comparable to the magnitude of the estimated isotropic component. In evaluating the uncertainty, we consider the following factors: correlation between the isotropic component and other components, mislocation of the centroid, and unmodelled earth structure.

4.1 Effect of correlation between the isotropic component and other components

Fig. 1 shows a comparison of the data and synthetics computed for the moment tensor solution obtained by the analysis of the normal-mode data. We now consider the effect of the choice of the period band on the results of the moment tensor inversion. In each case, we assume that the source time function is a step function.

Fig. 2(a) shows the dependence of the isotropic component obtained by the inversion on the period band chosen. For example, as shown at the bottom of the figure, using data in the period band from about 480–580 s leads to an isotropic moment of −7.7 per cent. On the other hand, using data in the period band from about 630–800 s leads, as shown at the top of Fig. 2(a), to an isotropic moment of +4.4 per cent. Thus, depending on the period band chosen for the inversion, we can obtain an isotropic moment ranging between about −8 per cent and +4 per cent.

To see which of these values should be considered more reliable, we consider the correlation between the isotropic component and the other components. Fig. 2(b) shows the maximum absolute value of the correlation coefficient between the isotropic component and the other components for each solution. In most cases, the vertical CLVD component has the largest correlation with the isotropic component. We obtain a small correlation between the isotropic component and the other components, and hence a more reliable estimate of the isotropic component, using normal-mode data at periods longer than 500 s, and choosing a wide period band, say up to 1000 s. When we use a narrow band, the correlation coefficient becomes large, and hence the solution becomes unreliable.

In Fig. 3(a), we plot the estimated isotropic components as a function of the maximum absolute value of the correlation coefficient between the isotropic component and the other components. The solution shown in Table 3, which is obtained by the analysis of the normal-mode data in the period band between 550 and 1000 s, is the one for which the maximum absolute value of the correlation coefficient is the smallest. When we show the results for other earthquakes later, we present the solution obtained using the Green's function computed for model 1066A, for which the maximum absolute value of the correlation coefficient between the isotropic component and the other components is the smallest. Note that the isotropic components with negative signs, which are implosive, appear when the correlation is large. Since they disappear when the correlation decreases, they are artefacts due to contamination due to correlation with the other components. Thus, it is essential to reduce the correlation between the

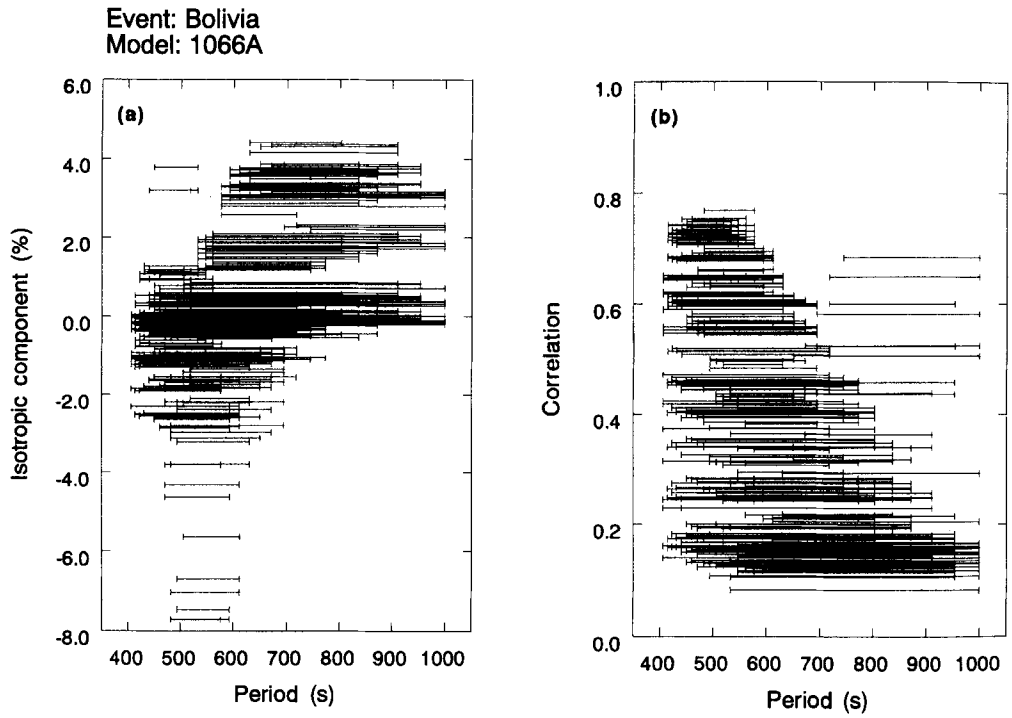

Figure 2. (a) The isotropic components determined for the Bolivia earthquake for the various period bands employed for the inversion. The isotropic components are presented as a percentage of the deviatoric seismic moment. (b) The maximum absolute value of the correlation coefficient between the isotropic component and the other components for each of the period bands used for the inversion.

Table 3. The moment tensor solutions of the Bolivia, Fiji and Japan Sea earthquakes.

Event	Bolivia			
Analysis	(a)	(b)	(c)	(d)
Period band	550-1000 s	20-250 s	50-100 s	250-500 s
M_{rr}	-0.74±0.03	-0.48±0.04	-0.26±0.05	-0.70±0.06
$M_{\theta\theta}$	0.97±0.05	0.48±0.04	0.39±0.06	0.70±0.08
$M_{\phi\phi}$	-0.06±0.05	-0.10±0.04	-0.07±0.05	-0.02±0.07
$M_{r\theta}$	-2.95±0.02	-1.80±0.02	-1.22±0.04	-2.73±0.03
$M_{r\phi}$	0.01±0.03	0.06±0.01	0.02±0.02	0.19±0.02
$M_{\theta\phi}$	-0.53±0.03	-0.32±0.02	-0.11±0.03	0.04±0.03
I	1.7±0.7%	-1.7±1.0%	1.7±3.8%	-0.3±2.3%
ε	0.04±0.03	0.05±0.04	0.07±0.09	0.00±0.05
V. R.	94.4%	87.2%	31.6%	80.0%
Event	Fiji			
Analysis	(a)	(b)	(c)	(d)
Period band	530-750 s	20-250 s	50-100 s	140-290 s
M_{rr}	-1.14±0.05	-1.17±0.09	-0.76±0.05	-1.24±0.07
$M_{\theta\theta}$	-0.12±0.09	0.48±0.11	0.02±0.05	0.01±0.09
$M_{\phi\phi}$	1.10±0.07	0.83±0.14	1.04±0.06	0.79±0.10
$M_{r\theta}$	-0.13±0.06	-0.20±0.05	0.01±0.03	0.06±0.02
$M_{r\phi}$	-2.54±0.04	-1.78±0.03	-1.92±0.04	-1.82±0.03
$M_{\theta\phi}$	1.38±0.08	1.10±0.06	1.11±0.03	1.16±0.03
I	-1.6±1.0%	1.8±2.8%	4.0±1.9%	-6.0±3.3%
ε	0.11±0.05	0.03±0.14	0.10±0.05	0.04±0.07
V. R.	95.0%	80.0%	52.3%	69.9%
Event	Japan Sea			
Analysis	(a)	(b)	(c)	(d)
Period band	470-550 s	20-250 s	50-100 s	140-290 s
M_{rr}	0.96±0.26	0.63±0.18	-0.43±0.17	0.19±0.21
$M_{\theta\theta}$	4.57±0.33	3.46±0.18	3.45±0.19	4.48±0.31
$M_{\phi\phi}$	-6.32±0.37	-2.59±0.22	-4.28±0.25	-4.78±0.37
$M_{r\theta}$	2.52±0.18	2.02±0.07	2.19±0.11	2.47±0.07
$M_{r\phi}$	-8.56±0.16	-5.86±0.09	-6.98±0.15	-8.33±0.12
$M_{\theta\phi}$	-3.49±0.28	-2.84±0.13	-1.86±0.11	-2.77±0.13
I	-2.2±1.4%	6.5±1.4%	-4.6±1.8%	-0.3±2.4%
ε	-0.15±0.06	-0.06±.04	-0.18±0.05	-0.16±0.06
V. R.	94.3%	79.6%	57.0%	76.9%

The unit is 10^{21}, 10^{20}, and 10^{19} N·m for the Bolivia, Fiji, and Japan Sea earthquakes, respectively. (a) Normal mode analysis; (b) P and SH waveform analysis; (c) CMT inversion of long period body waves; (d) CMT inversion of long period surface waves. I is the isotropic component specified as a percentage of the deviatoric seismic moment. V. R. is the variance reduction obtained by each solution.

isotropic component and other components to obtain a reliable estimate of the isotropic component.

Note also that there are many different solutions whose correlation coefficients are small (say less than 0.3), and that the magnitude of the estimated isotropic components for these solutions varies from about 0 to 4 per cent of the seismic moment. We consider this spread as the uncertainty of the determination of the isotropic component. Thus, we consider the value presented in Table 3 for the Bolivia earthquake (1.7 per cent) to be insignificant.

4.2 Effect of centroid location

We fixed the centroid location in the normal-mode analyses, which may have biased the solution. In order to evaluate the magnitude of this bias, we change the centroid location by 10 km in all three directions (vertical, east–west, north–south), and perform inversion for each location. The period band is the same shown in Table 3. Fig. 3(b) shows the estimated isotropic component for each location. The magnitudes of the isotropic components fluctuate by about ±1.5 per cent of the deviatoric seismic moment, although the correlation does not

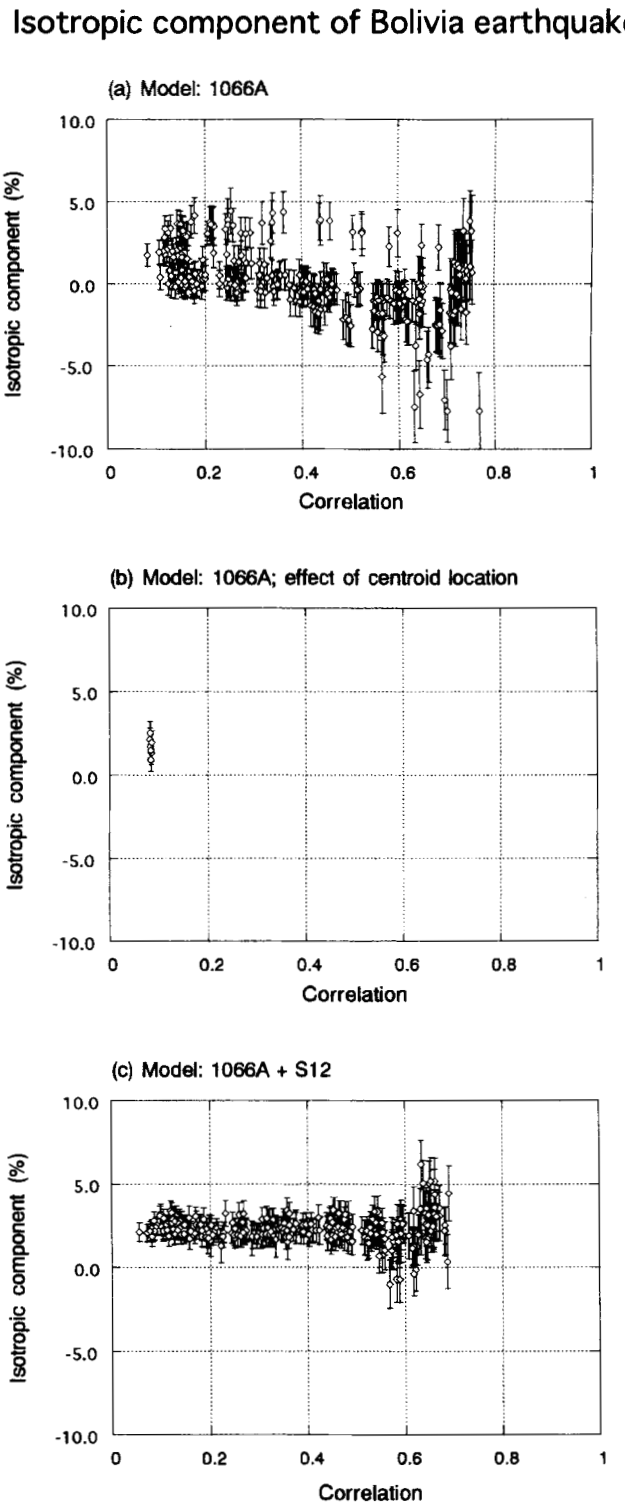

Figure 3. Evaluation of the uncertainty of the isotropic component obtained by the analysis of normal-mode data for the Bolivia earthquake. (a) The isotropic components determined by normal-mode data in various period bands, shown in Fig. 2(a). The horizontal axis shows the maximum absolute value of the correlation coefficient between the isotropic component and the other components for each solution. The isotropic component is specified as a percentage of the deviatoric seismic moments. (b) The isotropic components determined for six different centroid locations with the solution given in Table 3. (c) The same as (a), except that the earth model is S12-WM13.

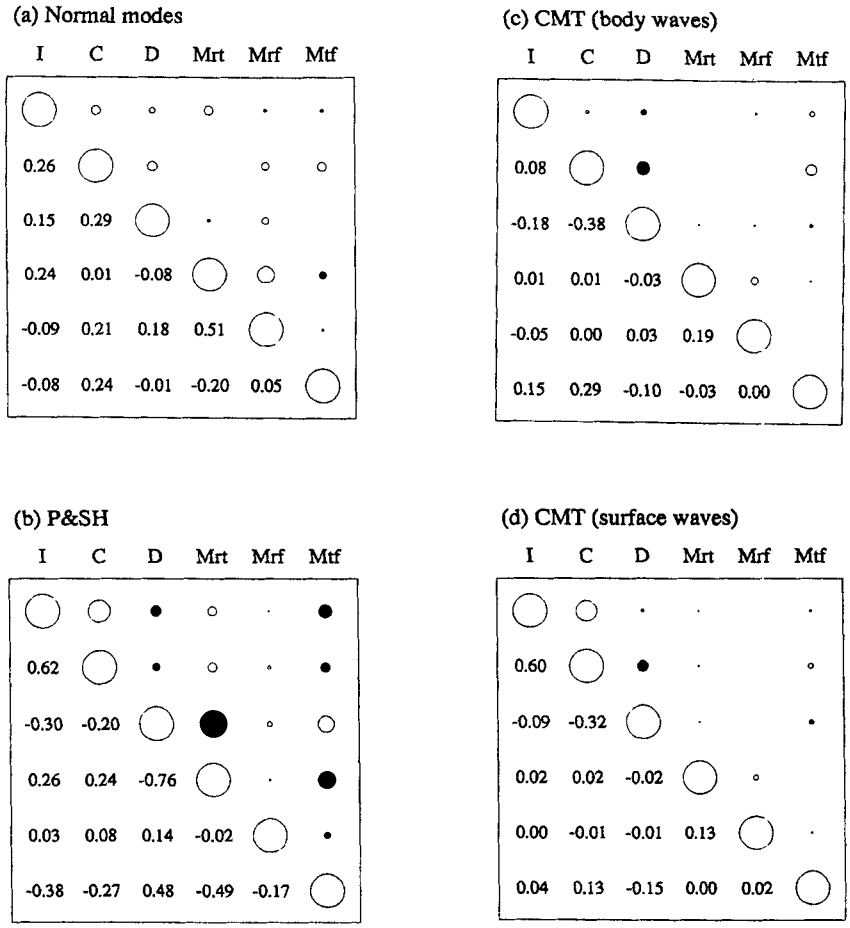

Figure 4. The correlation matrices corresponding to the solutions for the Fiji earthquake shown in Table 3. The diameters of the circles are proportional to the magnitudes of the correlation coefficients. The solid and open circles indicate negative and positive values, respectively.

change significantly. We consider this fluctuation as the uncertainty due to the error of the centroid location.

4.3 Effect of 3-D earth structure

Although we included the effect of the earth's rotation and its elliptical figure in computing the Green's functions, we did not include the effect of the 3-D seismic-velocity structure. We now conduct inversion using Green's functions computed for the laterally heterogeneous model S12-WM13 (Su, Woodward & Dziewonski 1994) with the spherically symmetric part of 1066A, and empirically investigate the effect of the 3-D seismic velocity structure. We scale the lateral heterogeneity of *P*-wave velocity, *S*-wave velocity and density according to $d \ln v_p / d \ln v_s = 0.8$ and $d \ln \rho / d \ln v_s = 0.4$. We fully consider the coupling between multiplets due to the laterally heterogeneous structure using the same trial functions as mentioned above.

Fig. 3(c) shows the estimated isotropic components. The spread of the estimates becomes narrower than in the analyses using the Green's function computed for 1066A. The variance reduction obtained by S12-WM13 is 2 per cent larger (measured as a percentage of the total variance of the observed seismograms) than that obtained for 1066A (Table 4). The narrower spread of the estimates is partially due to this better variance reduction, since the effect of the unmodelled earth structure is expected to decrease. This suggests that it is important to consider the effect of 3-D earth structure to obtain a precise estimate of the isotropic component. Because the magnitudes of the isotropic components whose correlation coefficients with other components are small are comparable to the uncertainty due to the centroid location shown above, it is difficult to conclude that the estimated isotropic component is convincingly significant.

Table 4. Variance reduction.

Model	Event				
	Bolivia	Fiji	Japan Sea	Banda Sea	South of Honshu
1066A	94.9%	96.6%	94.7%	90.9%	86.7%
S12_WM13	96.9%	96.7%	95.5%	95.3%	90.2%

The averages of the variance reductions obtained by the solutions shown in Fig. 3(a), (c), 5(a), (c), 7(a), (c), 9(a), (c), and 11(a), (c) are shown, respectively.

We summarize the results of our analyses for the Bolivia earthquake: no significant isotropic component is observed, and the magnitude of the isotropic component is at most 5 per cent of the deviatoric seismic moment if it exists at all.

5 RESULTS FOR OTHER EARTHQUAKES

We show above that the normal-mode data provide a precise estimate of the isotropic component. Here, we present the

results of the normal-mode analyses for the other deep earthquakes. Figs 4 and 5 and Table 3 give the results for the Fiji earthquake; Figs 6 and 7 and Table 3 for the Japan Sea earthquake; Figs 8 and 9 and Table 5 for the Banda Sea earthquake; Figs 10 and 11 and Table 5 for the South of Honshu earthquake. The results of the broad-band analyses are also presented for the Fiji and Japan Sea earthquakes.

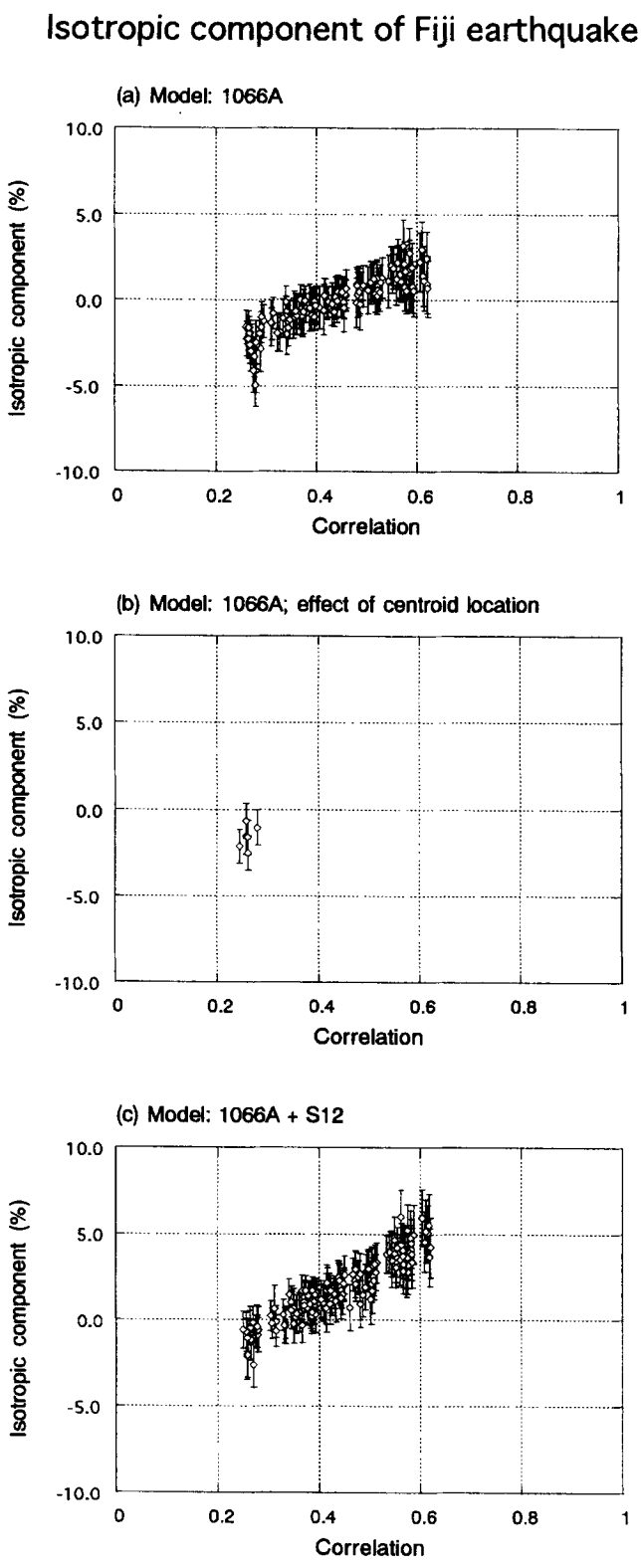

Figure 5. Evaluation of the uncertainty of the isotropic component obtained by the normal-mode data for the Fiji earthquake. The details are the same as in Fig. 3.

All of the magnitudes of the isotropic components estimated by the normal-mode data are less than two standard deviations (Tables 3 and 5), which suggests that no significant isotropic component exists for these earthquakes.

5.1 Normal-mode analyses

5.1.1 Correlation between the isotropic component and the other components

As in the analysis for the Bolivia earthquake, we vary the period bands of the normal-mode data used in the inversion to examine the uncertainty of our estimates. The solutions shown in Tables 3 and 5 for each event are those for which the maximum absolute value of the correlation coefficient between the isotropic component and the other components is the smallest. The period bands employed to obtain these solutions are also shown in Tables 3 and 5.

The correlation coefficients between the isotropic component and the other components are not as small as those for the Bolivia earthquake (Figs 4a, 6a, 8 and 10; see also Fig. 3d in Paper I). As we show in Fig. 2(b), it is necessary to use a broad period band, up to say 1000 s, to reduce the correlation. Since the S/N ratio decreases considerably at long periods for the other events, we cannot use data at periods up to 1000 s. The longest periods used are 750, 590, 650 and 580 s for the Fiji, Japan Sea, Banda Sea and South of Honshu earthquakes, respectively. Thus the correlation coefficients are not as small as those for the Bolivia earthquake.

5.1.2 Uncertainty of the estimated isotropic components

Although the correlation between the isotropic component and the other components is not as small as that for the Bolivia earthquake, judging from the results shown in Fig. 3, the spread of the estimates is unlikely to change significantly as long as the maximum absolute value of the correlation coefficients is less than 0.3. We therefore consider the spread of the solutions for which the maximum absolute values of the correlation coefficients are less than, or around, 0.3 as the uncertainty of the isotropic component.

For the Fiji earthquake, the magnitudes of the estimated isotropic components vary from -1 to -5 per cent of the deviatoric seismic moment, when the maximum absolute value

Table 5. The moment tensor solutions of the Banda Sea and South of Honshu earthquakes.

Event	Banda Sea	South of Honshu
Period band	550-650 s	480-560 s
M_{rr}	-1.15±0.05	-0.34±0.12
$M_{\theta\theta}$	-0.16±0.05	0.25±0.10
$M_{\phi\phi}$	1.32±0.07	-0.15±0.13
$M_{r\theta}$	0.79±0.04	0.62±0.05
$M_{r\phi}$	0.00±0.05	-1.23±0.06
$M_{\theta\phi}$	1.09±0.05	-0.20±0.05
I	0.3±1.6%	-5.3±4.4%
V. R.	92.4%	86.3%

The unit is 10^{20} N·m.

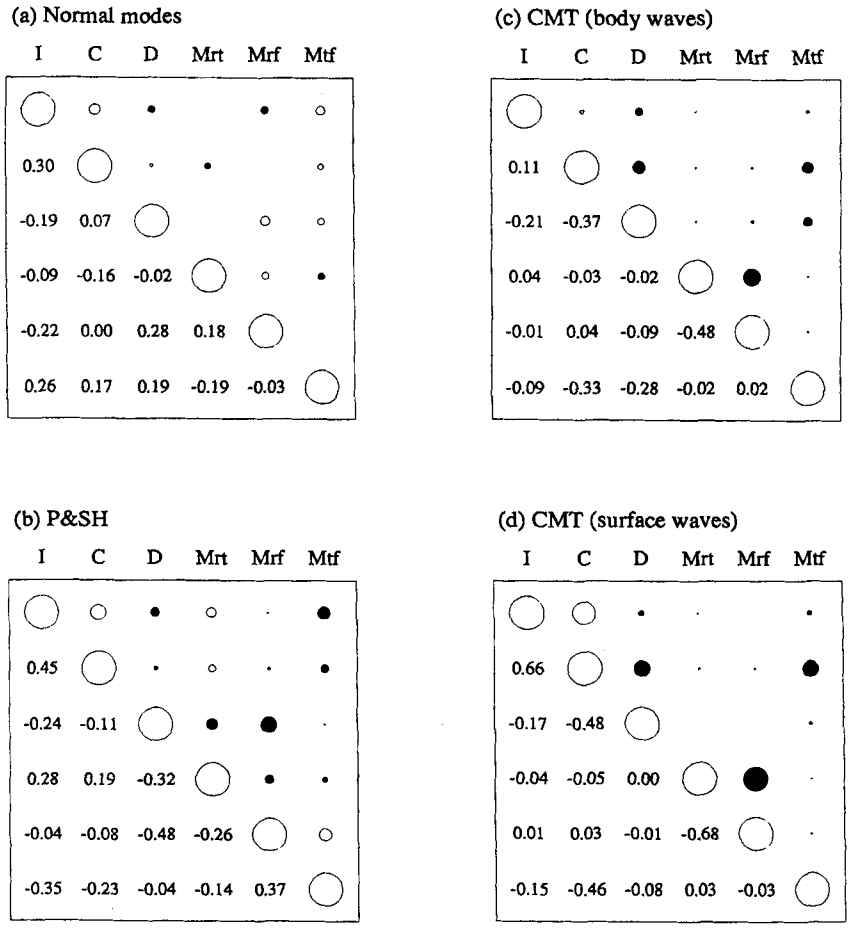

Figure 6. The correlation matrices corresponding to the solutions for the Japan Sea earthquake shown in Table 3. The details are the same as in Fig. 4.

of the correlation coefficients is less than 0.3 (Fig. 5a). Taking into account the uncertainty due to the error of the centroid location shown in Fig. 5(b), this value is insignificant. The spread of the estimates does not change significantly when we consider the effect of 3-D earth structure (compare Figs 5a and c). This seems to be partially due to the fact that the variance reduction obtained for S12-WM13 is comparable to that obtained for 1066A (Table 4). We thus find that no significant isotropic component is observed for the Fiji earthquake; the magnitude is at most 5 per cent of the deviatoric seismic moment.

For the Japan Sea earthquake (Fig. 7), based on the spread of the estimates for which the maximum absolute value of the correlation coefficient is around 0.3, no significant isotropic component is observed; the magnitude is at most 4 per cent of the deviatoric seismic moment.

For the Banda Sea earthquake (Fig. 9), the spread of the estimates becomes narrower when we consider the effect of 3-D earth structure of S12-WM13, as was also seen in the analyses for the Bolivia earthquake. This is likely to be partially due to the larger variance reduction obtained for S12-WM13 than for 1066A (Table 4). Judging from the spread of the estimates for which the maximum absolute value of the correlation coefficient is less than 0.3, no significant isotropic component exists; the magnitude is at most 5 per cent of the deviatoric seismic moment.

Fig. 11(a) shows that, for the South of Honshu earthquake, there is an apparently implosive component whose magnitude reaches 15 per cent of the deviatoric seismic moment when the maximum absolute value of the correlation coefficient is large (say 0.5–0.6). However, since this disappears when the correlation decreases, it is an artefact. Such artefacts can be expected to be larger for this earthquake, since the variance reduction is smaller than for the other earthquakes (Table 4). This small variance reduction is partially due to not employing the first portions of the observed seismograms to avoid problems due to non-linearity of the instrument and to using a longer time-series than in the analyses for the Fiji and Japan Sea earthquakes. This suggests that, in determining the isotropic component, it is desirable, if possible, to restrict the time-series to only R1 and R2.

The spread of the estimates is narrower in Fig. 11(c) than in (a), which implies that the effect of the unmodelled earth structure is smaller in Fig. 11(c). This is consistent with the larger variance reduction obtained for S12-WM13 than for 1066A (Table 4). Thus, the estimates obtained for S12-WM13 seem more reliable; judging from the spread of the estimates for which the maximum absolute value of the correlation coefficient is around 0.3 in Fig. 11(c), the magnitude of the isotropic component is likely to be less than 5 per cent of the deviatoric seismic moment, although the constraint is weaker than in the analyses of the other earthquakes.

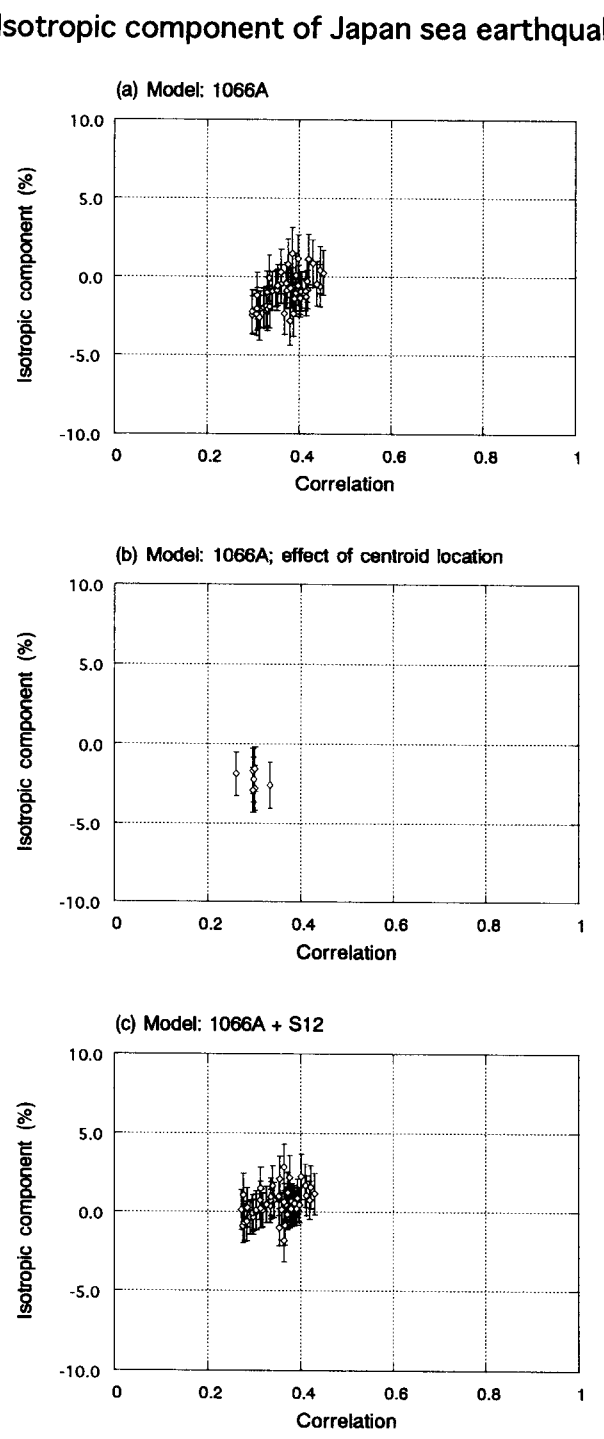

Figure 7. Evaluation of the uncertainty of the isotropic component obtained by the normal-mode data for the Japan Sea earthquake. The details are the same as in Fig. 3.

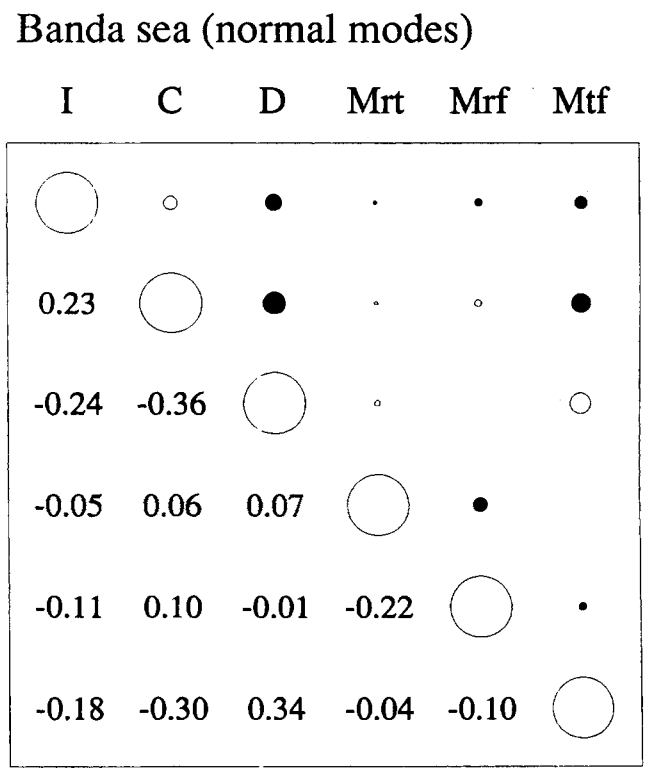

Figure 8. The correlation matrix corresponding to the solution for the Banda Sea earthquake shown in Table 5. The details are the same as in Fig. 4.

5.2 Broad-band analyses

5.2.1 Non-double-couple component, ε

For the Fiji earthquake, the values of ε are small in all analyses (Table 3), which suggests that there is no large non-double-couple deviatoric component for this earthquake.

In contrast to the results for the Bolivia and Fiji earthquakes, the absolute values of ε of the Japan Sea earthquake are relatively large (Table 3), which suggests the possible existence of a non-double-couple deviatoric component for this earthquake.

5.2.2 Isotropic component

Figs 4(b)–(d) and 6(b)–(d) show the correlation matrices obtained in the broad-band analyses for the Fiji and Japan Sea earthquakes, respectively. As is the case in the analyses for the Bolivia earthquake (Fig. 3 in Paper I), the correlation coefficients between the isotropic component and the other components are large for the analyses of the *P* and *SH* waves and the long-period surface-wave data, and are small in the analyses of the long-period body-wave data.

The magnitude of the isotropic component determined by the analyses of the long-period body-wave data is larger than two standard deviations for these earthquakes (Table 3). However, we consider these values insignificant, because, as shown above, the actual uncertainty of the isotropic component determined by the normal-mode analyses is larger than two standard deviations, and because the uncertainty of the analyses of the long-period body-wave data seems still larger, since the effect of unmodelled earth structure can be expected to be larger due to the smaller variance reduction (Table 3).

6 DISCUSSION

We showed above that no significant isotropic component was obtained by the normal-mode analyses. We precisely estimated the upper limit of the isotropic component, and showed that

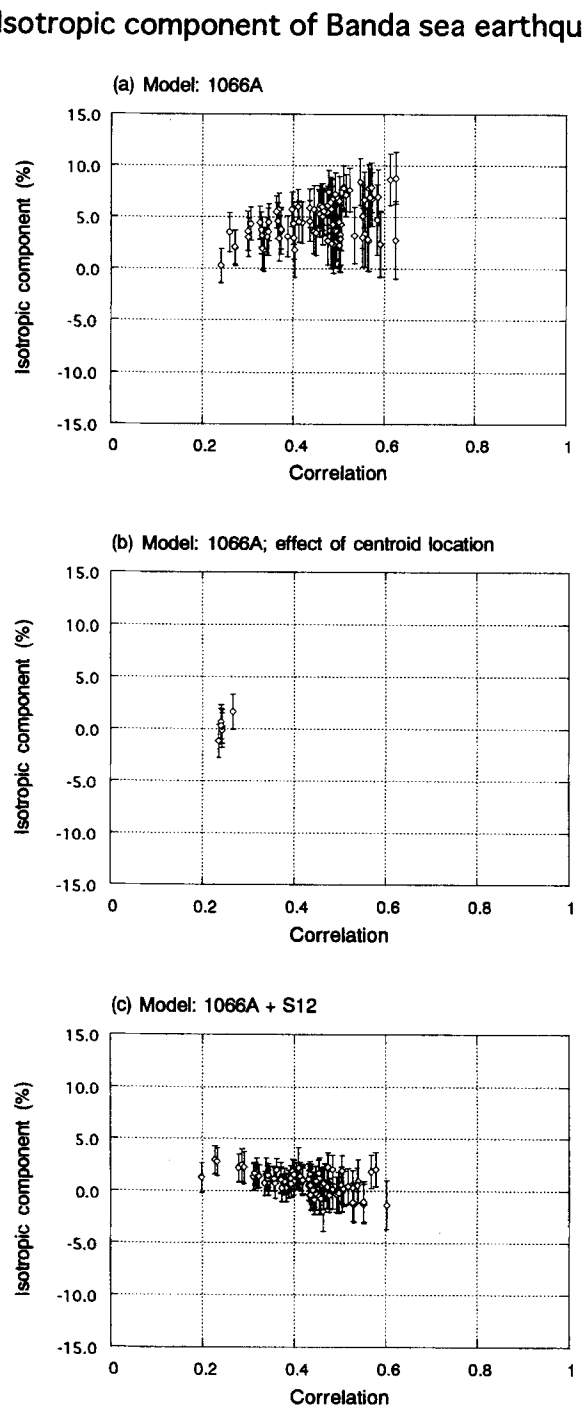

Figure 9. Evaluation of the uncertainty of the isotropic component obtained by the normal-mode data for the Banda Sea earthquake. The details are the same as in Fig. 3.

its magnitude is at most 5 per cent of the deviatoric seismic moment. This is consistent with the results of Kawakatsu (1991, 1996), who analysed long-period body-wave data in the period band between 50 and 100 s. These results suggest that no large isotropic component exists for deep earthquakes in the period band between 50 and 1000 s.

The magnitudes of the estimated isotropic components are comparable to the uncertainty due to the error of the centroid location (assumed to be on the order of 10 km in the above

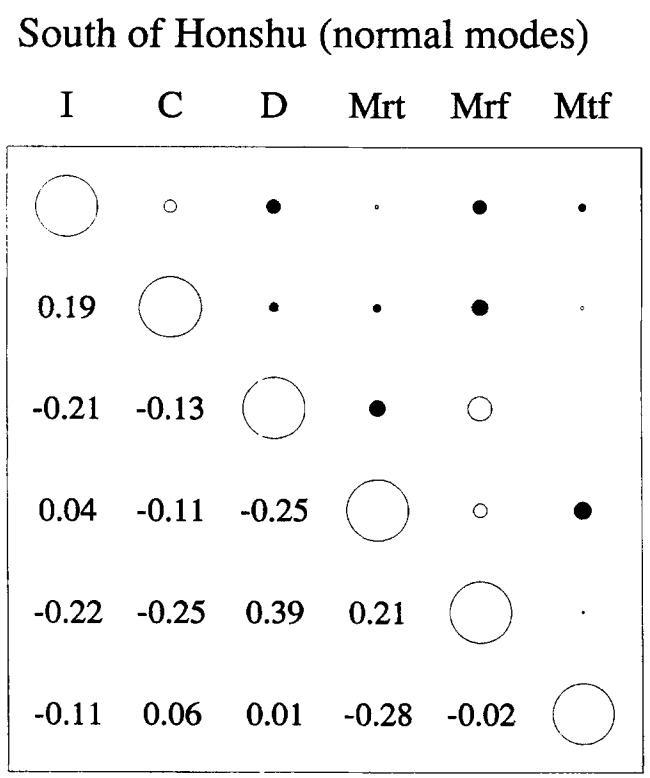

Figure 10. The correlation matrix corresponding to the solution for the South of Honshu earthquake shown in Table 5. The details are the same as in Fig. 4.

analyses). It is desirable to make a precise estimate of the centroid location and its error based on accurate calculations. Recently, Hara (1996) has developed such an algorithm, in which the direct solution method is used in computing synthetic seismograms. Moreover, this new algorithm can be applied to simultaneous inversion of earthquake source parameters and 3-D earth structure. The application of this new algorithm will provide a precise and reliable estimate of the centroid location and its error and then make it possible to conduct a more precise determination of the isotropic component in the near future.

No large non-double-couple deviatoric component was observed for the Bolivia and Fiji earthquakes, while a small but relatively consistent non-double-couple deviatoric component was found for the Japan Sea earthquake. Kawasaki & Tanimoto (1981) suggested that anisotropic seismic velocity structure around the source region could cause the significant non-double-couple component. Anderson (1987) pointed out the possible existence of anisotropy within a subducting slab. Here, we consider the possibility that anisotropic structure could be the cause of the non-double-couple component of the Japan Sea earthquake.

There are two candidates for the main mineral around the source of the Japan Sea earthquake, which occurred at a depth of 478 km. If the equilibrium phase-change occurs, the material around the source will mainly consist of β spinel (e.g. Katsura & Ito 1989). The other candidate is metastable olivine, which recent seismological studies suggest may exist within subducting slabs (Iidaka & Suetsugu 1992; Wiens, McGuire & Shore 1993; Iidaka & Furukawa 1994). The anisotropy of these minerals (Kumazawa & Anderson 1969; Sawamoto *et al.* 1984)

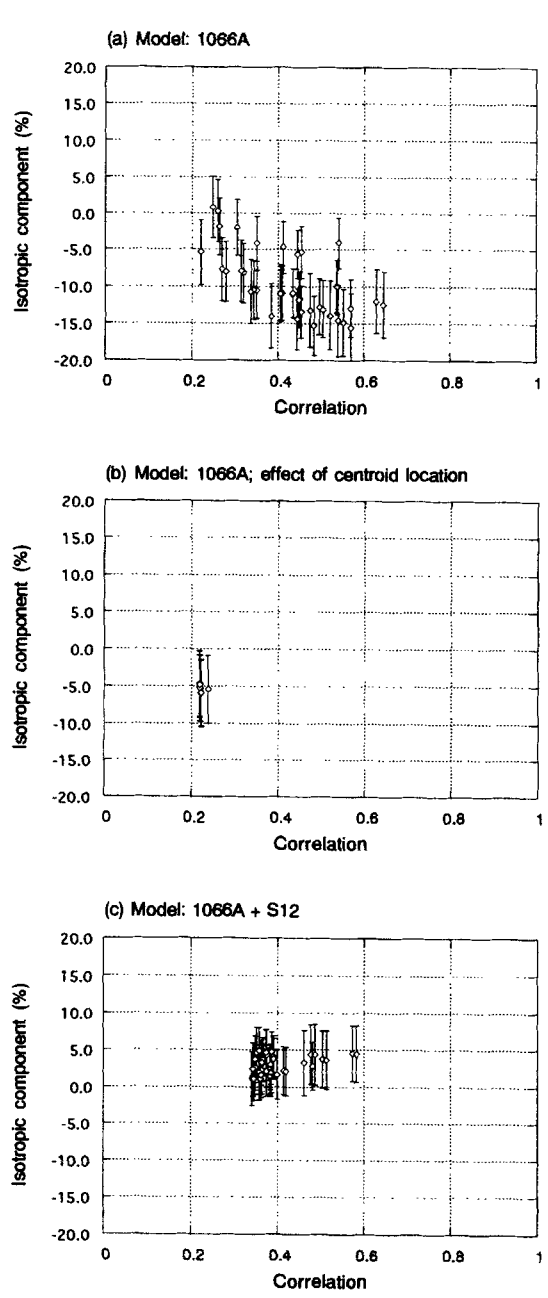

Figure 11. Evaluation of the uncertainty of the isotropic component obtained by the normal-mode data for the South of Honshu earthquake. The details are the same as in Fig. 3.

could produce non-double-couple components whose magnitudes are comparable to that observed for the Japan Sea earthquake.

However, if this was the case, an isotropic component whose magnitude is 5–10 per cent of the deviatoric seismic moment would also be observed. This is not supported by our estimation of the upper limit of the isotropic component; it is thus unlikely that anisotropic seismic-velocity structure could cause the observed non-double-couple component.

Kuge & Kawakatsu (1992) suggested that, for the 1987 northern Sea of Japan earthquake (May 7), the observed non-double-couple component might be produced by sub-events whose focal mechanisms were double couples with different orientations that occurred at almost the same time. We prefer this idea as the cause of the non-double-couple deviatoric component of the Japan Sea earthquake.

Since there is no significant isotropic component and non-double-couple component for the Bolivia and Fiji earthquakes, there is no evidence for a significant volumetric change, or for an anisotropic structure around the source region for these earthquakes.

Based on these results, using the upper limit of the isotropic component, we can calculate the upper limit of the possible volume change during the ruptures of these earthquakes. Using the values of the bulk modulus of 1066A, the upper limits are estimated to be about 0.6 and 0.07 km^3 for the Bolivia and Fiji earthquakes, respectively.

Recently, transformational faulting has been proposed as the physical mechanism responsible for deep earthquakes (Green & Burnley 1989; Green *et al.* 1990; Kirby, Durham & Stern 1991). In this theory, deep earthquakes are caused by a shear instability due to a rapid phase change of metastable olivine within a thin layer. We assume that the density change due to the phase change is 8 per cent in the following discussion. This value corresponds to $\alpha \rightarrow \beta$ transformation of olivine (e.g. Ringwood 1991), and is, of course, smaller than those due to the $\alpha \rightarrow \gamma$ or $\alpha \rightarrow$ (perovskite + magnesiowustite) transformation. Therefore, our values give an upper limit of the volume associated with the phase change, since the isotropic moment is proportional to (density change) × (associated volume). The upper limit of the volume of the mantle material that would transform into the denser phase is about 7 km^3 for the Bolivia earthquake and 0.9 km^3 for the Fiji earthquake.

For these earthquakes, the fault dimensions are estimated as 30×50 km^2 for the Bolivia earthquake (e.g. Silver *et al.* 1995) and 50×65 km^2 for the Fiji earthquake (Wiens *et al.* 1994). Then, using our estimate of the upper limit of the volume, we can estimate the average thickness of the mantle material that would transform during the rupture. The thickness is about 5 m for the Bolivia earthquake and 30 cm for the Fiji earthquake. The factors of the values may change, because we assume that the mantle material that would transform distributes uniformly, and because a fraction of the mantle material may transform before the rupture initiates, as is expected from the theory of transformational faulting. However, their orders are not likely to vary significantly. Thus, if a rapid phase change occurs during the ruptures of deep earthquakes, the mantle material that transforms is likely to be confined within an extremely thin layer; for example, the ratio of the thickness to the fault dimension would be on the order of $1:10^5$ for the Fiji earthquake.

7 CONCLUSION

We precisely determine the isotropic components of large deep-focus earthquakes by inversion for all six components of their moment tensors using normal-mode data. We carefully evaluate the uncertainty due to the correlation between the isotropic component and the other components, the error of the centroid location, and 3-D earth structure. We show that it is possible to determine the isotropic component independently by analyses of normal-mode data at periods longer than 500 s, and that better constraints on the isotropic component can be

obtained by using Green's functions for the present 3-D earth model.

We find that there is no significant isotropic component for any of the earthquakes we studied; the magnitude of the isotropic component is at most 5 per cent of the deviatoric seismic moment. Thus, if rapid phase changes occur during the rupture of deep earthquakes, the mantle material that transformed should be confined within an extremely thin layer.

A broad-band analysis of body-wave and surface-wave data showed that there is a relatively consistent non-double-couple deviatoric component of the moment tensor for the 1994 Japan Sea earthquake. This non-double-couple component appears to be due to the complex source process, such as double-couple subevents with different source mechanisms that occurred at almost the same time.

ACKNOWLEDGMENTS

We thank Wei-jia Su for providing us with the model parameters of model S12-WM13. We thank Phil Cummins for valuable comments. This research was supported by the Earthquake Research Institute cooperative research program (1994-G2-10 and 1995-G2-04).

REFERENCES

Anderson, D.L., 1987. Thermally induced phase changes, lateral heterogeneity of the mantle, continental roots, and deep slab anomalies, *J. geophys. Res.*, **92,** 13 968–13 980.

Dziewonski, A.M. & Gilbert, F., 1974. Temporal variation of the seismic moment tensor and the evidence of precursive compression for two deep earthquakes, *Nature* **247,** 185–188.

Geller, R.J., Hara, T., Tsuboi, S. & Ohminato, T., 1990. A new algorithm for waveform inversion using a laterally heterogeneous starting model, in *Seismological Society of Japan Fall Meeting,* 296 (in Japanese).

Giardini, D., 1983. Regional deviation of earthquake source mechanisms from the 'double-couple' model in *Earthquakes: Theory and Interpretation,* pp. 345–353, eds. Kanamori, H. & Bosch, E., North-Holland, Amsterdam.

Giardini, D., 1984. Systematic analysis of deep seismicity: 200 centroid-moment tensor solutions for earthquakes between 1977 and 1980, *Geophys. J. R. astr. Soc.,* **77,** 883–914.

Gilbert, F. & Dziewonski, A.M., 1975. An application of normal mode theory to the retrieval of structure parameters and source mechanisms from seismic spectra, *Phil. Trans. R. Soc. Lond.,* A, **278,** 187–269.

Green, H.W. & Burnley, P.C., 1989. A new self-organizing mechanism for deep-focus earthquakes, *Nature,* **341,** 733–737.

Green, H.W., Young, T.E., Walker, D. & Scholz, C.H., 1990. Anticrack-associated faulting at very high pressure in natural olivine, *Nature,* **348,** 720–722.

Hara, T., 1996. An efficient algorithm for iterative waveform inversion for 3-D earth structure and earthquake source parameters, in *Japan Earth and Planetary Science Joint Meeting,* 336 (in Japanese with English abstract).

Hara, T., Tsuboi, S. & Geller, R.J., 1991. Inversion for laterally heterogeneous earth structure using a laterally heterogeneous starting model: preliminary results, *Geophys. J. Int.,* **104,** 523–540.

Hara, T., Tsuboi, S. & Geller, R.J., 1993. Inversion for laterally heterogeneous upper mantle *S*-wave velocity structure using iterative waveform inversion, *Geophys. J. Int.,* **115,** 667–698.

Hara, T., Kuge, K. & Kawakatsu, H., 1995. Determination of the isotropic component of the 1994 Bolivia deep earthquake, *Geophys. Res. Lett.,* **22,** 2265–2268.

Iidaka, T. & Furukawa, Y., 1994. Double seismic zone for deep earthquakes in the Izu–Bonin subduction zone, *Science,* **263,** 1116–1118.

Iidaka, T. & Suetsugu, D., 1992. Seismological evidence for metastable olivine inside a subducting slab, *Nature,* **356,** 593–595.

Katsura, T. & Ito, E., 1989. The system Mg_2SiO_4–Fe_2SiO_4 at high pressures and temperatures: precise determination of stabilities of olivine, modified spinel, and spinel, *J. geophys. Res.,* **94,** 15 663–15 670.

Kawakatsu, H., 1991. Insignificant isotropic component in the moment tensor of deep earthquakes, *Nature,* **351,** 50–53.

Kawakatsu, H., 1996. Observability of the isotropic component of a moment tensor, *Geophys. J. Int.,* **126,** 525–544.

Kawasaki, I. & Tanimoto, T., 1981. Radiation patterns of body waves due to the seismic dislocation occurring in an anisotropic source medium, *Bull. seism. Soc. Am.,* **71,** 37–50.

Kirby, S.H., Durham, W.B. & Stern, L.A., 1991. Mantle phase changes and deep-earthquake faulting in subducting lithosphere, *Science,* **252,** 216–225.

Kuge, K. & Kawakatsu, H., 1990. Analysis of a deep 'non-double couple' earthquake using very broadband data, *Geophys. Res. Lett.,* **17,** 227–230.

Kuge, K. & Kawakatsu, H., 1992. Deep and intermediate-depth non-double couple earthquakes: interpretation of moment tensor inversions using various passbands of very broadband seismic data, *Geophys. J. Int.,* **111,** 589–606.

Kuge, K. & Kawakatsu, H., 1993. Significance of non-double couple components of deep and intermediate-depth earthquakes: Implications from moment tensor inversions of long-period seismic waves, *Phys. Earth. planet. Inter.,* **75,** 243–266.

Kumazawa, M. & Anderson, O.R., 1969. Elastic moduli, pressure derivatives, and temperature derivatives, of single-crystal olivine and single-crystal forsterite, *J. geophys. Res.,* **74,** 5961–5972.

Mendiguren, J.A. & Aki, K. 1978. Source mechanism of the deep Colombian earthquake of 1970 July 31 from the free oscillation data, *Geophys. J. R. astr. Soc.,* **55,** 539–556.

Okal, E., 1996. Radial modes from the great 1994 Bolivian earthquake: No evidence for an isotropic component to the source, *Geophys. Res. Lett.,* **23,** 431–434.

Okal, E.A. & Geller, R.J., 1979. On the observability of isotropic seismic sources: The July 31, 1970 Colombian earthquake, *Phys. Earth. planet. Inter.,* **18,** 176–196.

Randall, M.J. & Knopoff, L., 1970. The mechanism at the focus of deep earthquakes, *J. geophys. Res.,* **75,** 4965–4976.

Ringwood, A.E., 1991. Phase transformation and their bearing on the constitution and dynamics of the mantle, *Geochim. Cosmochim. Acta,* **55,** 2083–2110.

Sawamoto, H., Weidner, D.J., Sasaki, S. & Kumazawa, M., 1984. Single-crystal elastic properties of the modified spinel (beta) phase of magnesium orthosilicate, *Science,* **224,** 749–751.

Silver, P.G., Beck, S.L., Wallace, T.C., Meade, C., Myers, S.C., James, D.E. & Kuehnel, R., 1995. Rupture characteristics of the deep Bolivian earthquake of 9 June 1994 and the mechanism of deep-focus earthquakes, *Science,* **268,** 69–73.

Su, W.-J., Woodward, R.L. & Dziewonski, A.M., 1994. Degree 12 model of shear velocity heterogeneity in the mantle, *J. geophys. Res.,* **99,** 6945–6980.

Vasco, D.W. & Johnson, L.R., 1989. Inversion of waveforms for extreme source models with an application to the isotropic moment tensor component, *Geophys. J.,* **97,** 1–18.

Wiens, D.A., McGuire, J.J. & Shore, P.J., 1993. Evidence for transformational faulting from a deep double seismic zone in Tonga, *Nature,* **364,** 790–793.

Wiens, D.A., McGuire, J.J., Shore, P.J., Bevis, M.G., Draunidalo, K., Prasad, G. & Helu, S.P., 1994. A deep earthquake aftershock sequence and implications for the rupture mechanism of deep earthquakes, *Nature,* **372,** 540–543.

APPENDIX A: DISCRIMINATION BETWEEN THE ISOTROPIC COMPONENT AND THE VERTICAL CLVD COMPONENT USING NORMAL-MODE DATA

Kawakatsu (1996) suggested that it may be possible to distinguish the isotropic component from the vertical CLVD component using normal-mode data at periods longer than 500 s. In a previous paper (Hara *et al.* 1995), using normal-mode data in the period band between 550 and 1000 s, we showed that we can determine the isotropic component of the 1994 Bolivia earthquake independently from the other components. Here, we explain the reason why we can reduce the correlation between the isotropic component and the other components.

Of the five components of the moment tensor other than the isotropic component, the vertical CLVD component will have the largest correlation with the isotropic component. This is because both the isotropic component and the vertical CLVD component have the same radiation pattern with $m=0$, where m is the azimuthal order number. The excitation of the $m=0$ component of spheroidal normal modes for a laterally homogeneous earth model and a point source on the z-axis is proportional to

$$\frac{(2l+1)}{\omega_k^2}\left[M_{rr}\frac{dU}{dr}+(M_{\theta\theta}+M_{\phi\phi})\left(\frac{U}{r}-l(l+1)\frac{V}{2r}\right)\right],$$

where l is the angular order number, ω_k is the eigenfrequency, and U and V are the radial eigenfunctions.

In Fig. A1 we show the relative excitation of spheroidal modes due to an isotropic point source and a vertical CLVD point source located at a depth of 671 km [the excitation is normalized so that the maximum absolute value in Fig. A1(a) is 1]. While the magnitude of the relative excitation due to the isotropic component is less than 0.3 for almost all of the overtone modes (although we show only the values for the first and second overtones, this also holds for higher overtone modes), it is larger than 0.3 for most of the fundamental modes. Therefore, fundamental modes primarily constrain the isotropic component. However, at periods shorter than 500 s (above 2 mHz), the sign of the excitation due to the isotropic component is always positive, while that due to the vertical CLVD component is always negative. This causes a large correlation between the isotropic and vertical CLVD components.

On the other hand, at periods longer than 500 s (below 2 mHz), the sign of the excitation due to the vertical CLVD component changes from negative to positive. This is the reason for the decreased correlation between the isotropic and vertical CLVD components that allows them to be clearly distinguished using data at periods longer than 500 s. This is also the case for shallower (say, at a depth of 450 km) earthquakes.

The excitation of radial modes at periods longer than 500 s ($_0S_0$ and $_1S_0$) due to the isotropic component is larger than

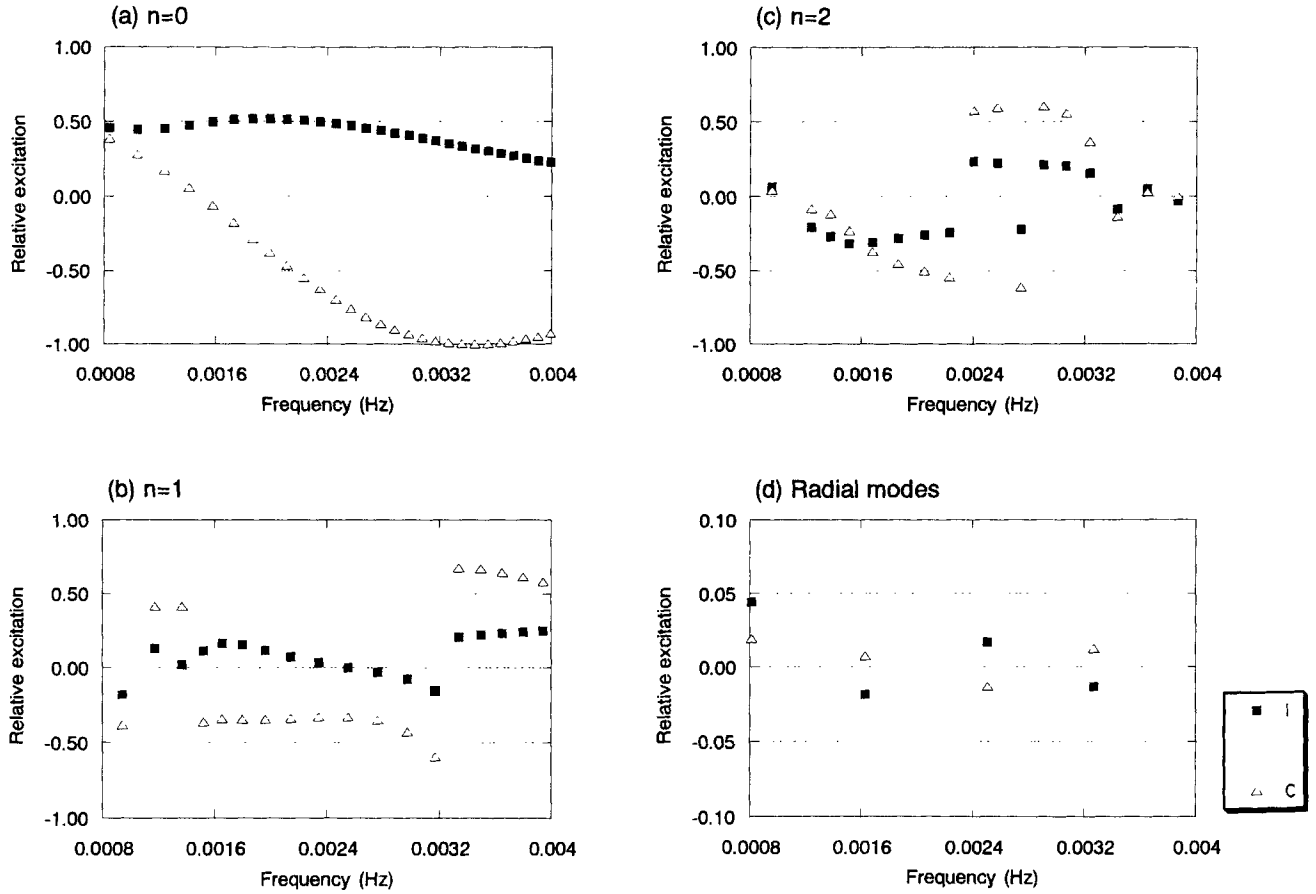

Figure A1. (a) The relative excitation of fundamental modes due to the isotropic (solid squares) and vertical CLVD component (open triangles); (b) first overtone modes; (c) second overtone modes; and (d) radial modes. The source is located at a depth of 671 km. The excitation is normalized so that the maximum absolute value in (a) is 1.

that due to the vertical CLVD component (Fig. A1d). Hence, these modes are sensitive to the isotropic component. Recently, Okal (1996) showed by an analysis of ${}_0S_0$ and ${}_1S_0$ that no significant isotropic component is observed for the Bolivia earthquake. Because the relative excitation of radial modes is much smaller than that of spheroidal modes [note that the vertical scale of Fig. A1(d) is one tenth of the other figures], and because, as discussed by Okal (1996), a very long time-series, say up to 80 days, is necessary for the analysis of ${}_0S_0$ because of its large quality factor, it is difficult to conduct a precise determination of the isotropic component using radial modes, except for very large earthquakes such as the Bolivia earthquake.